Journal of Engineering Physics and Thermophysics, Vol. 81, No. 1, 2008

DIAGNOSTICS OF RAPIDLY PROCEEDING PROCESSES IN FLUID AND PLASMA MECHANICS

N. A. Fomin

UDC 535.36

A brief description of the main methods used for diagnostics of rapidly proceeding processes in fluid and plasma mechanics is presented. In this description prominence is given to the optical methods of diagnostics and new techniques based on the use of digital laser technologies and statistical methods of measurement-data processing. Examples of application of the indicated methods and techniques, demonstrating their potentialities, are given.

Introduction. The study of rapidly proceeding processes in fluid and plasma physics and in the mechanics of liquids, gases, and plasma is necessary for solving many important engineering problems concerning the use of combustion and detonation processes, the propagation of shock waves, the provision of fire and explosion safety, hydrogen power, in the rocket and aircraft industry, and others. Since rapid processes cannot be measured directly, it is necessary to develop special methods for diagnostics of these processes and recording their parameters [1–4].

Over many years, such investigations were carried out predominantly with the use of optical methods of diagnostics because these methods offer numerous advantages, the most important of which is the possibility to perform highly informative are nondisturbing optical measurements with a high accuracy and a high spatial and temporal resolution [5–11].

A powerful impetus to the development of optical methods of diagnostics is the discovery of laser systems and the wide use of them in measurement practice [12–19]. The appearance of lasers has fostered the development of optical diagnostics with the use of spectral analysis, the Doppler effect, and speckle fields generated by a coherent radiation [20–23]. The discovery of these fields has made it possible to use digital systems for recording and processing of images. These systems radically changed the possibilities of quantitative measurements and description of complex tree-dimensional rapid processes occurring in many technological processes and new technical equipment. The formation of informative banks of data on complex phenomena by the results of millions and millions of quantitative measurements became possible when digital laser speckle technologies and new approaches to the statistical analysis of enormous files of experimental data with the use of a computer were developed [24].

Quantitative Methods of Diagnostics with the Use of Detectors and Tracers. The modern measurements of rapidly proceeding processes originate from the first attempts made in the distant past to visualize flows with the use of particles-tracers introduced into these flows. The results of such a visualization can be found even in ancient rock drawings. A scientific qualitative analysis of the indicated visualization was made in the Renaissance, in particular in illustrated treatises of Leonardo Da Vinci devoted, e.g., to the representation of vortex flows and even the blood flow in the arterial valves of the heart [24]. The first documented quantitative measurements, carried out with the use of tracers, date from 1689 [25]. These measurements were carried out by Van Leeuwenhoek and were also devoted to the anemometry of the blood flow; in this work, the tracers were blood elements — erythrocytes that are also used for measuring the blood flow with the use of modern digital measuring systems [26].

The first measurements of the velocity of a flow with the use of a detector were carried out by the engineer Pitot in 1732 (see [27]). He measured the flow of the river Seine in Paris. In the simplest cases, in accordance with the Bernoulli theorem, the velocity of a flow is determined by the differential height h in the tube of a water pressure gauge:

$$V = \left[2\,(p_0 - p)/\rho_{\text{air}}\right]^{1/2} = \left(2\rho_{H_2O} g h/\rho_{\text{air}}\right)^{1/2}.$$

A. V. Luikov Heat and Mass Transfer Institute, National Academy of Sciences of Belarus, 15 P. Brovka Str., Minsk, 220072, Belarus; email: fomin@hmti.ac.by. Translated from Inzhenerno-Fizicheskii Zhurnal, Vol. 81, No. 1, pp. 68–80, January–February, 2008. Original article submitted September 27, 2007.

 1062-0125/08/8101-0068©2008 Springer Science+Business Media, Inc.

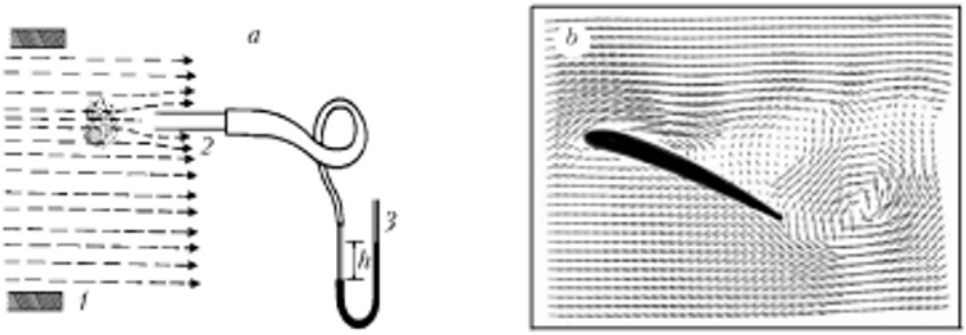

Fig. 1. Measurement of the velocity of flow with the use of a Pitot detector (a) and a velocity field reconstructed by an original Prandtl photography with the use of the autocorrelation-analysis data of [23] (b): 1) channel; 2) Pitot detector; 3) U-like pressure guide.

To carry out more exact measurements with the use of the Pitot technique, it is necessary to determine the influence of the compressibility, viscosity, turbulence, and many other parameters of a fluid on the velocity of its flow. However, in all the cases, the dynamic parameters of this technique remained low. The development of the hot-wire anemometry realized with the use of wire and film detectors made it possible to substantially improve the temporal resolution of such measurements. By the end of the 20th century, the time resolution of detectors used for this purpose (with commercial filaments of thickness 0.25 μm) reached 1 μsec and is continuously being improved at present with the use of nanotechnologies [28].

Even in the Prandtl works carried out early in the 20th century, repeated attempts have been made to carry out a qualitative anemometry of flows on the basis of analysis of the paths of visualizing particles. In this case, particles were uniformly introduced into the flow being investigated. In order for the velocities of particles to give a complete estimate of the flow, these particles should be fairly small. Particles of micron or even submicron sizes are usually used in this case; Doppler also used such particles in his measurements [14]. The anemometry based on the analysis of the motion of individual particles is called the particle tracking velocimetry in the modern English-language literature [24]. Figure 1 shows the field of a flow, reconstructed by Doctor Kompenhans (German Aerospace Center, Göttingen) from an original photography of Prandtl with the use of digital methods of image processing [23]. The modern tracing technique is based on the statistical analysis of the displacement of images of particles visualizing a flow for a definite time in the case where these particles are recorded in a definite plane on a photoplate or by a CCD camera (see Fig. 2).* The particles are illuminated by laser radiation forming, with the use of a cylindrical lens, a thin plane called the laser knife, which allows one to separate a two-dimensional measurement plane in a three-dimensional volume.

The thermodynamic temperature of fluids is usually measured with the use of different thermocouples and thermistors [29, 30]. The thermocouples have a larger dynamic range than the thermistors; however, the thermistors surpass the thermocouples in sensitivity by an order of magnitude. The frequency range of such detectors is substantially limited; this is true even for modern thermocouples of diameter 20–40 μm.

One of the most important parameters determined in the process of investigating rapidly proceeding processes is pressure. For measurement of this parameter, a number of broadband detectors of appropriate design have been developed [31]. In the general case, the pressure of a fluid is expressed in terms of nine components of the stress tensor and, in the simplest case, in terms of its diagonal elements. Detectors, in which the deformation of an elastic element, e.g., a piezocrystal, is used for obtaining an electric signal, have a wide application in such measurements [32]. These detectors process a good bandwidth-duration product since micron deformations are sufficient for polarization of their piezoelectric element; because of this, their sluggishness is not due to the displacement of the center of mass and is determined by the time of establishment of the deformation state. Academician R. I. Soloukhin fabricated and used

*This technique is called particle image velocimetry (PIV) and represents anemometry based on the analysis of particle images. Its digital analog is the Digital PIV (DPIV).

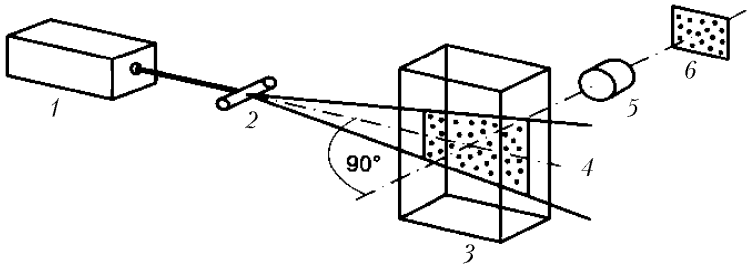

Fig. 2. Optical scheme of measuring the velocity of a flow by the PIV method: 1) probing laser; 2) cylindrical lens; 3) flow being investigated; 4) laser knife; 5) receiving objective; 6) plane of an image.

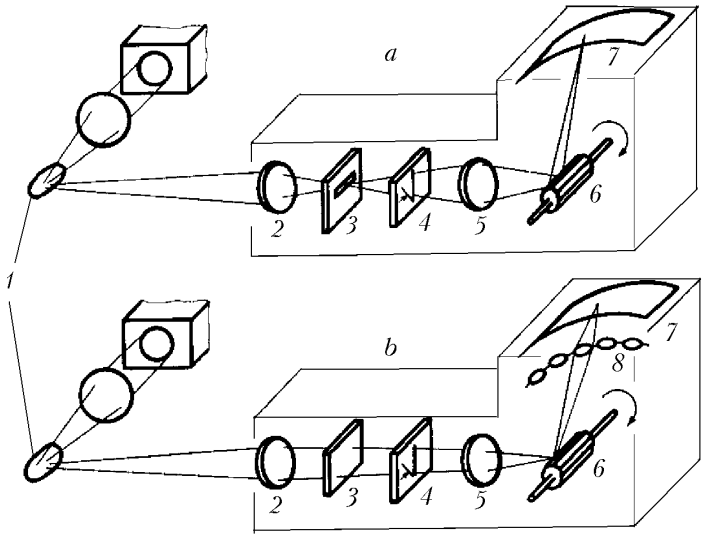

Fig. 3. Mechanical system with a rotating mirror for scanning of images of rapidly proceeding processes in the continuous regime (a) and in the regime of framing (b): 1) object being investigated; 2) objective forming an image; 3) slot (mask); 4) shutter; 5) receiving objective; 6) rotating mirror; 7) plane of image (cine film); 8) microobjective for formation of frames.

such detectors for measuring the pressure in the wake of shock waves [33]. In [34], a detector of this type with a matching amplifier, providing a temporal resolution of the order of several microseconds in measuring rapidly changing pressures, was described. The use of an acoustically matched absorbing rod in this detector makes it possible to eliminate the influence of the shock wave reflected from the face surfaces of the piezoelectric element and the spurious pulsations of the signal recorded.

The development of detectors for measuring heat flows was also fairly advantageous [35]. The use of distributed (e.g., liquid-crystal) indicators in optical methods made it possible to develop quantitative methods of measuring the stresses and pressure everywhere on the surface of the apparatus being tested [36]. At present, along with liquid crystals, pressure-sensitive paints and luminophors that change their properties under the action of stresses are widely used in such measurements [37, 38].

Sources of Probe Radiation and Methods of Recording Images of Rapidly Proceeding Processes. The visualization of rapidly proceeding processes calls for pulsed or pulsed-periodic light sources generating a high-power short pulses. Well before lasers were developed, Mach and Salcher recorded the supersonic flow near a flying bullet with the use of a spark light source [39, 40]. By the time of laser development in 1960, the visualization of rapidly proceeding processes was carried out with the use of light sources based on pulsed electric discharges, exploding wires, and different flash lamps [41]. In this case, the duration of an illumination pulse was, at best, several units of

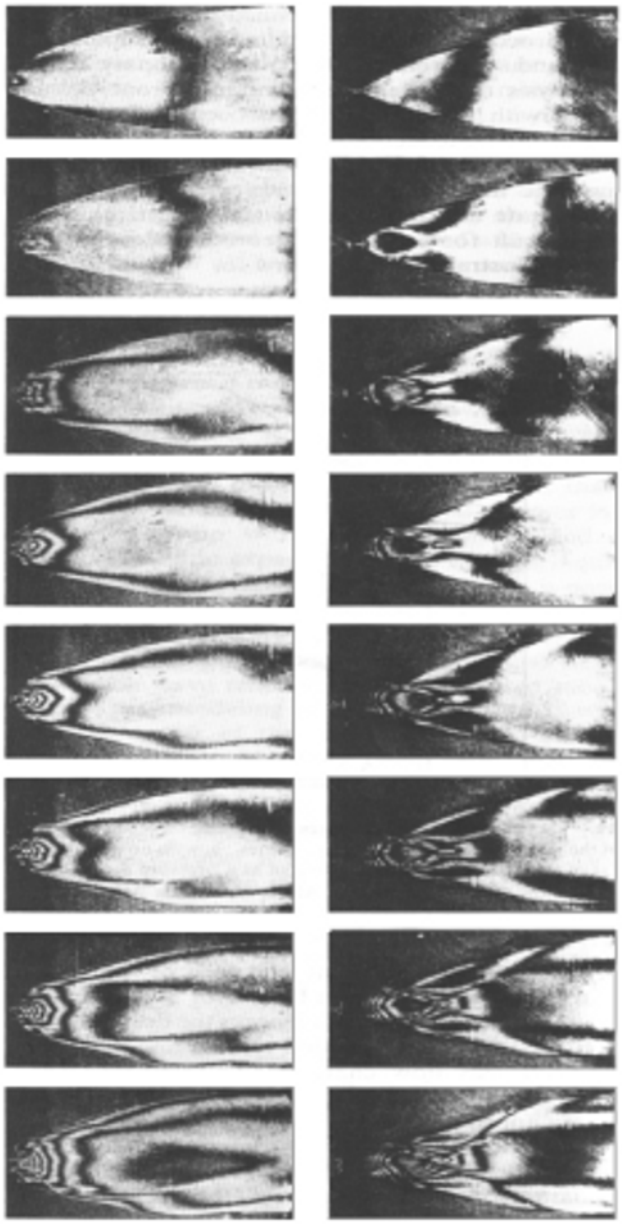

Fig. 4. Time sequence (from the top down) of the visualizing patterns of the shock-wave actuation of the nozzle in a gas-dynamic mixing laser, obtained with the use of a Mickelson interferometer, in the case of central injection of a radiating gas (at the left) and in the case of injection through the side walls (at the right) [42].

a nanosecond and the radiation energy reached several hundreds of millijoules. The monochromatism and coherence of laser light sources made it possible to develop new methods of diagnostics of rapidly proceeding processes. In experiments on gas dynamics, high-power lasers are traditionally used, which is explained by the low sensitivity of high-resolution holographic plates. For example an Nd-YAG laser with a frequency doubling has a power sufficient for visualization of flows; at a wavelength λ = 532 nm, it produces pairs of radiation pulses of repetition rate 10–20 Hz with a pulse separation $\Delta t \geq 1$ μsec. The indicated wavelength is convenient for many reasons. The optical sensitivity of both the photographic plates and the digital CCD cameras corresponds to this wavelength. Moreover, in many CCD cameras the number of green cells is two times larger than the number of red or blue cells [24]. The duration of each generation pulse is 50 nsec, which is sufficient for obtaining "instantaneous" (frozen) images of particles even for rapid

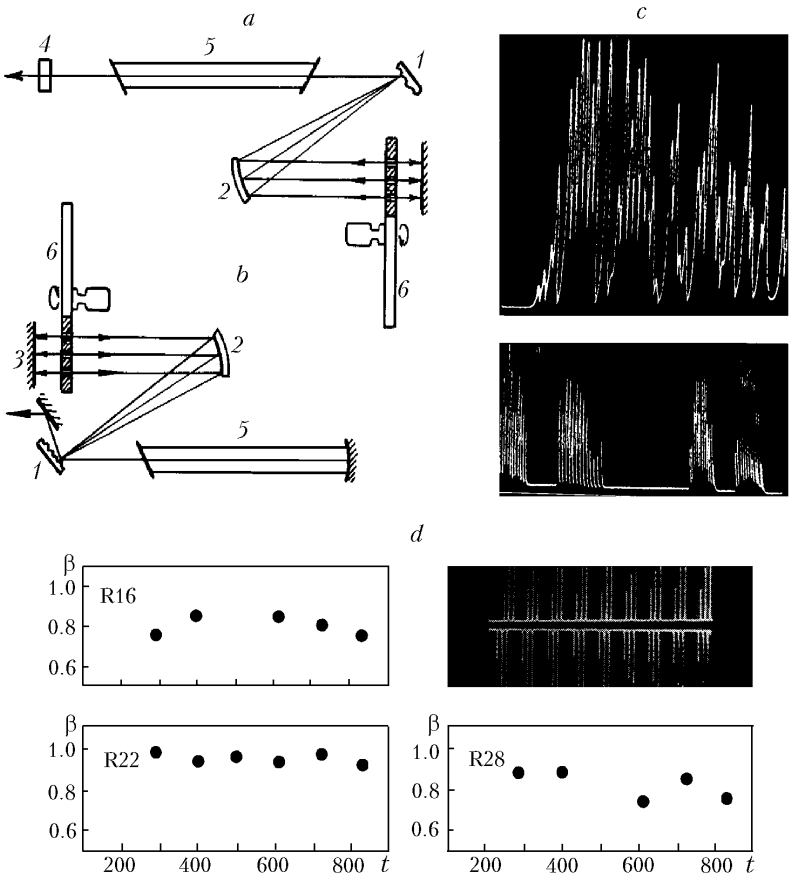

Fig. 5. Two variants of the Jacobi–Soloukhin laser spectrograph with coupling of radiation from the cavity with the use of a semireflecting mirror (a) and a diffraction grating (b); generation spectra of a spectrograph based on carbon monoxide measured at 5 μm (at the top) and a spectrograph based on carbon dioxide measured at 10.4 and 9.6 μm (c) and results of measurement of the translational temperature in the wake of the front of a shock wave with the use of this spectrograph in the case of simultaneous recording of the time change in the absorption coefficients β in the lines R16, R22, and R28 of the 001–100 transition of carbon dioxide (d): 1) diffraction grating; 2) parabolic mirror; 3) plane-parallel mirror; 4) semireflecting mirror; 5) electric-discharge tube; 6) rotating disk with slots. t, μsec.

processes. The wavelength of ruby lasers (Cr^{3+}, λ = 694 nm) is less suitable for this purpose; however, these lasers possess, on average, a higher power and can generate radiation in both the Q-switching mode (Δt = 50–100 nsec) and in the multibeam free running mode (Δt = 1 msec).

Lasers based on copper vapor have similar output parameters. The wavelength of such a laser can be 510.6 nm or 578.2 nm. The energy of an individual pulse is equal to approximately 10 mJ at a pulse duration of 15–50 nsec. The repetition frequency of pulses can be very high — several tens of kilohertzs, which provides a very high average power — several tens of watts in the pulse-periodic regime.

A numerous number of continuous lasers can be used for visualization of comparatively slow flows, e.g., liquid flows. He–Ne lasers (λ = 633 nm) are used most frequently for these purposes. These lasers have a milliwatt power. Argon lasers (Ar^{+}, λ = 514 nm, 488 nm) possess a much higher power — as high as several tens of watts. Radiation pulses of continuous lasers can be formed as a result of an external modulation, e.g., with the use of an acousto-optic modulator or even a rotating disk with slots.

Semiconductor lasers represent fairly promising and quickly progressing radiation sources; their power, at a good optical quality, can reach several terms of milliwatts in the continuous TEM_{00} mode. These lasers can be modulated by a pulse voltage. In [24], tables of wavelength of many other modern lasers are presented.

A large number of mechanical, electrooptical, and mechanical-electrooptical techniques have been developed for recording of sequences of flow images (Fig. 3). Rapidly rotating mirrors provide a scanning speed as high as 1–2 mln frames in a second at a high spatial resolution determined by the recording medium. Figure 4 shows a sequence of interference images of the process of actuation of a nozzle by a shock wave, obtained with the use of an SFR photodetector with a scanning speed of 500,000 frames in a second [42]. Electrooptical methods of scanning make it possible to substantially increase the speed of recording of processes; however, they do not provide a high spatial resolution. The optical Cranz–Schardin systems allow one to further increase the speed of scanning at a high optical quality of images; however, the number of frames in such systems is limited (see [13]).

Spectral Methods of Diagnostics. One of the first applications of lasers for investigating rapidly proceeding processes was laser Doppler anemometry (see [12–14]). Along with this anemometry, the development of lasers with a rapid restructuring of the generation spectrum has opened up new opportunities for diagnostics of rapid processes on the basis of analysis of the resonance and quasi-resonance absorption of a frequency-controlled probe radiation in media being investigated. Different modifications of CO_2 lasers are used as probe-radiation sources in measurements of CO_2- and CO-containing media. The generation spectrum of such lasers can be slowly changed by changing the angle of inclination of the diffraction grating. In the laser spectrograph with a spatial resolution of lasing lines, developed by U. A. Jacobi and R. I. Soloukhin (Fig. 5), lasing lines are rapidly restructured by selective suppression of the undesirable lines with the use of combinations of rotating and immovable masks placed in the laser cavity. With the use of this spectrograph, "rapid" measurements of the vibrational and translational temperatures were carried out in experiments on equilibrium and nonequlibrium flows in shock tubes [42, 43].

Quantitative Diagnostics of Flows with the Use of Digital Laser Speckle Technologies. The above-described methods of visualization of high-velocity flows in fluid mechanics were primarily developed within the framework of optical interferometry and holography and are realized with the use of photographic systems for fixation of images. An evident drawback of these systems is that the negative obtained must be photoprocessed under special conditions for a certain time [44]. The situation changes radically when speckle fields used for visualization of the indicated flows are recorded with the use of digital system [45–51]. In this case, instead of the optical processing of a specklogram, its digital cross-correlational analysis is carried out, which makes it possible to determine the vector of the average displacement of speckles in each subzone of the digital specklogram stored in the memory of a computer. Actually, let the distribution of the intensity of a speckle field recorded with the use of a CCD camera having $M \times N$ elementary cells be described by the function $I_i(m, n)$, where i is the number of an exposure, $m \in (1, 2, ..., M)$, and $n \in (1, 2, ..., N)$. Comparing two images, one can determine their cross-correlational function $\mathbb{R}_{ij}(\Delta\mathbf{S}) = \langle I_i(\mathbf{S}) I_j(\mathbf{S} + \Delta\mathbf{S}) \rangle$:

$$\mathbb{R}_{ij}(p, q) = \frac{MN}{(M-p)(N-q)} \left[\frac{\sum_{m=1}^{M-p} \sum_{n=1}^{N-q} I_i(m, n) I_j(m+p, n+q)}{\sum_{m=1}^{M} \sum_{n=1}^{N} I_i(m, n) I_j(m, n)} \right]. \quad (1)$$

Figure 6 shows the main elements of an experimental setup for digital recording of images of a flow with the use of a computer. At present, a large number of different solid-body matrices* are used for conversion of radiation into an electric signal. The image of a flow is formed in each pixel of a CCD camera by its receiving optics as a result of the total scattering of radiation by the visualizing particles in the solid angle Ω in the volume shown in Fig. 7. The intensity of the radiation fallen on a pixel during its open (working) state is converted into a charge, whose value is proportional to the total number of photons fallen on the pixel and the information on which is stored in the

*CCD is a photosensitive device with charge coupling, CMOS is a complementary metal oxide semiconductor, CID is a device with an injected charge.

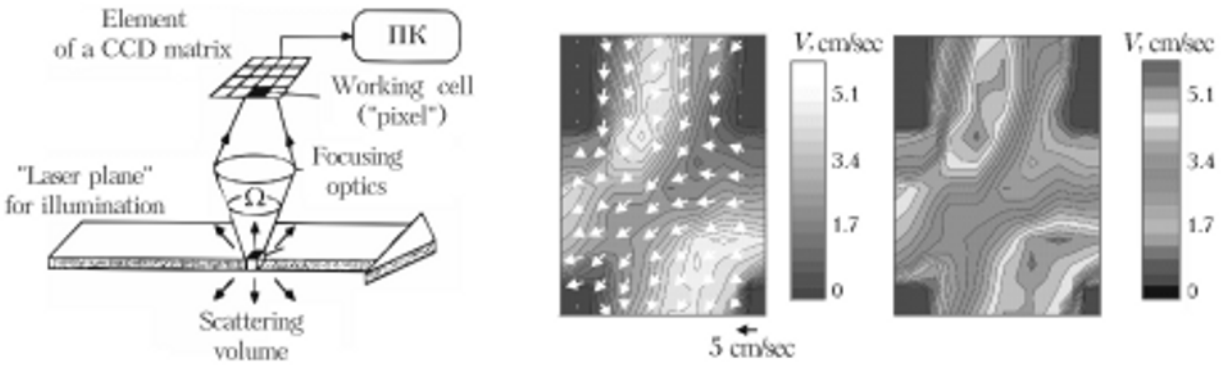

Fig. 6. Schematic diagram of the digital recording of speckle fields and elements of an experimental micro-DPIV setup (at the left) and fragments of a microflow in a fuel-element model (at the right).

memory of a computer or in an intermediate data-storage medium during the closed state of the pixel. A characteristic feature of the CCD elements is that they can accumulate a large charge (10,000–100,000 electrons), which allows them to measure the intensity of radiation in a large dynamic range. In such measurements, the noise sources are the dark current caused by the thermal effects in a pixel, the noises caused by the recording of a signal, the parasitic scattering of radiation by the walls of the channels and by foreign particles and surfaces, the background radiation arising in the process of measurements, etc. The intrinsic noises of the pixels are very sensitive to an increase in the temperature of a medium; they increase by two times when the medium is heated by 6–7^{o}C. Matrices with a cryogenic cooling have a very low intrinsic noise — as low as one electron in a second per pixel. The noises of the recording in the television standard can reach several hundreds of electrons per pixel for the period of recording of a charge. The noises of the recording can be decreased to several electrons per pixel for the time of recording of a charge by optimization of the recording process and with the use of elements cooled by electrons due to the Peltier effect. Thus, the dynamic range of measurements of the intensity of radiation can reach 16 bit per pixel, which corresponds to 65,000 gradations of the radiation intensity recorded in each cell.

The main feature of a modern CCD matrix is that it contains a large number of sensitive elements. At present, pixels have a size smaller than $10 \times 10\,\mu$m, and the number of pixels in a matrix exceeds 100^2 per square millimeter; this resolution is comparable with the spatial resolution of highly sensitive photoemulsions and lower by about more than an order of magnitude than the resolution of the best low-sensitivity holographic emulsions [44].

Figure 6 shows a scheme of digital recording of images. In this figure, fragments of microflows in a hydrogen-power fuel cell, calculated by digital laser speckle photographies, are presented. The software of the experiment [51] makes it possible to reconstruct as much as 250,000 velocity vectors in the two-dimensional region of a flow of size 20 × 30 mm, photographed with an optical magnification equal to unity. The dimensions of the region being investigated can be decreased by 10–100 times with the use of the corresponding microoptical equipment and an optical magnification. In the configuration presented, the spatial resolution in the measurement plane (m, n) comprises about 100 μm. Along the coordinate coincident with the optical ray, the averaging is performed over the depth of the flow, which is equal to 1 mm in this case.

Main Methods and Algorithms of Processing of Digital Images. As was noted above, a digital image is analyzed with the use of a two-dimensional cross-correlational function of two successive images, calculated by (1). For this purpose, the image obtained is divided into small subregions, in each of which the cross-correlational function is calculated as a function of the coordinates of this subregion (m, n) (Fig. 7).

The cross-correlational function, determined with account for the experimental noises in each such zone of the spectrogram $\tilde{\sigma}(m, n)$, represents a convolution of the corresponding regions of images:

$$\mathbb{R}_{1,2}(m, n) = I_1(m, n) \otimes I_2(m, n) + \tilde{\sigma}(m, n) . \qquad (2)$$

In the Fourier plane, this relation has the form

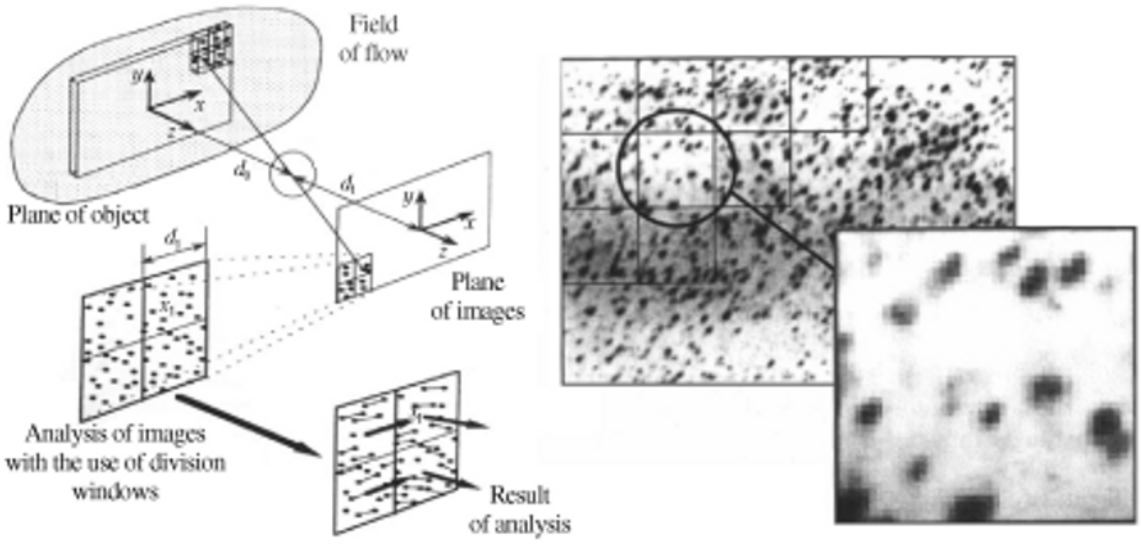

Fig. 7. Recording of particles in the plane of an image and division of a CCD matrix into averaging windows.

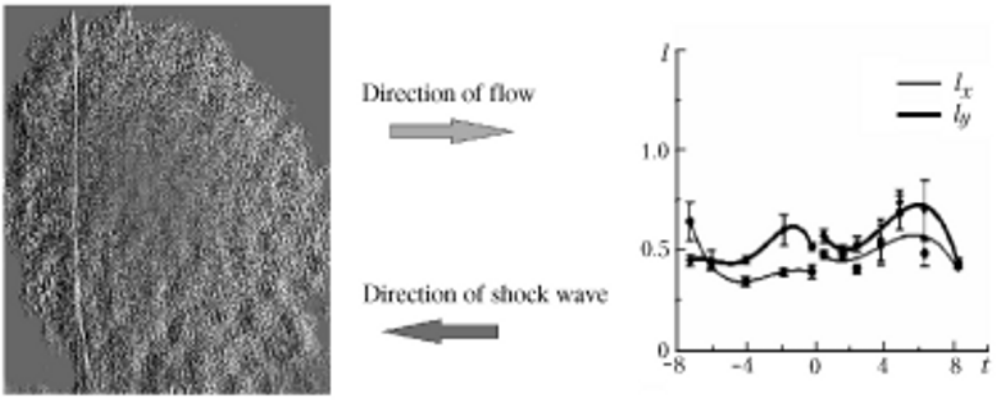

Fig. 8. Specklogram of a turbulent flow interacting with a shock wave and evolution of the longitudinal (l_x) and transverse (l_y) Kolmogorov scales calculated by this specklogram. l_x, l_y, mm. t, μsec.

$$\mathbb{F}\left\{\mathbb{R}_{1,2}\right\}(u, \nu) = \mathbb{F}\left\{I_1\right\}(u, \nu)\cdot\mathbb{F}\left\{I_2\right\}(u, \nu) + \sigma(u, \nu)\,, \tag{3}$$

where $\sigma(u, \nu)$ is the corresponding noise in the Fourier plane. The strategy of the cross-correlational analysis of successive images is that the desired function $\mathbb{R}_{1,2}(m, n)$ is determined by filtration of the noises of specklograms in both the initial physical plane and the Fourier plane for the subregions $I_1(m, n)$ and $I_2(m, n)$. Evidently, the desired function can be estimated using relation (2):

$$\left\{\widetilde{\mathbb{R}}_{1,2}\right\}(m, n) = \mathbb{F}^{-1}\left\{\mathbb{F}\left\{\widetilde{I}_1\right\}(u, \nu)\cdot\mathbb{F}\left\{\widetilde{I}_2\right\}(u, \nu)\right\}, \tag{4}$$

where $\widetilde{I}_1$ and $\widetilde{I}_2$ are the filtrated specklograms. Some methods of such filtration are described in [23].

Correlational functions and the contrast of speckle fields can be calculated on modern personal computers in the time intervals between the successive frames in the process of recording of digital images in the television standard (at a frequency of 25 Hz, this interval is equal to 40 msec) with the use of even CCD cameras having an ultimately high resolution, which makes it possible to perform the diagnostics of flows in real time [50].

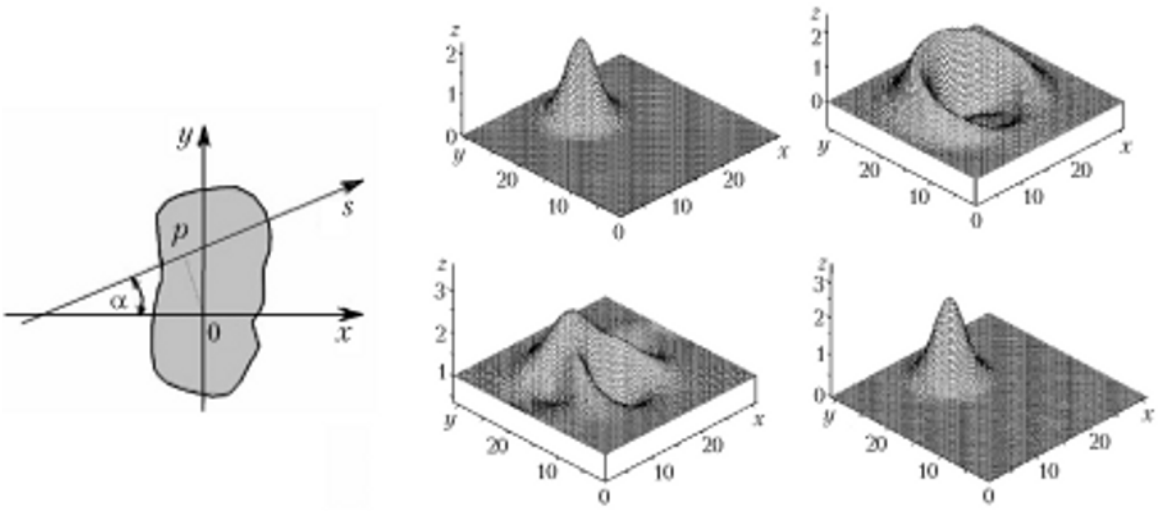

Fig. 9. Geometry of the integral Radon transform and fragments of the density distribution of a three-dimensional flow along the coordinates x and y in relative units calculated by the data of the small-aspect-angle speckle tomography performed in [52, 53].

For illustration of the potentialities of the statistical processing of a large body of information on a flow in real time, we will consider the use of speckle technologies for the reconstruction of the evolution of the microscale of turbulence in the process of propagation of a shock wave [21]. Such a reconstruction is shown in Fig. 8; which indicates that the technique used provides a high spatial resolution reaching 20–30 μm in this case. This is much smaller than the Kolmogorov scale (500–1000 μm) for the experimental conditions being considered.

Tomographic Methods of Investigating Three-Dimensional Flows. The above-described line-in-sight laser probing of optically transparent media is an integral visualization technique making possible the obtaining of two-dimensional images of three-dimensional flows:

$$F_{s_i} = \int_{s_i} f(x, y, z)\, ds_i , \tag{5}$$

where the function $f(x, y, z)$ describes the response of an optical system to the probing of a medium. In this case, the data on a flow along the optical path are integrated, which makes the analysis of the structure of a complex three-dimensional flow difficult.* The summarized beam is conventionally represented by the projection angle α (see Fig. 9). Then

$$F_{s_i} = F_s(\alpha, p) \quad \text{and} \quad F_\alpha(p) = \iint f(x, y)\, \delta(x \sin\alpha + y \cos\alpha - p_0)\, dxdy , \tag{6}$$

where $p = x \sin\alpha + y \cos\alpha$ is the so-called impact parameter and δ is the delta function.

At small angles of deflection ($\varepsilon << 1$), the desired three-dimensional distribution can be constructed stage-by-stage. At first, a set of two-dimensional desired functions $f(x, y)$ are determined for different coordinates z_1 and, then, the desired three-dimensional function $f(x, y, z)$ is constructed. In this case, a summarized two-dimensional beam is obtained by integration over the s_i-th ray

*The two-dimensional visualization can be also performed with the use of light sheet techniques (PIV, PLIF, LIF, and others) involving illumination of a flow by a laser plane (laser knife). These techniques are free of the above-indicated drawbacks associated with the averaging of data along the optical path. However, they offer no way to obtain information on a three-dimensional flow as a whole and provide the obtaining of data only in a separated plane.

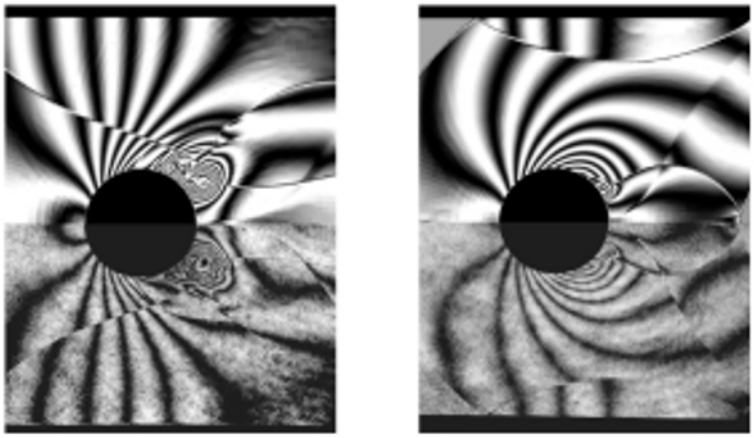

Fig. 10. Comparison of the calculation data on a three-dimensional shock-wave flow in the form of synthesized interference bands (upper part of the interferogram) with the experimental data (lower part of the interferogram) obtained for two successive instants of time [53].

$$F(\alpha, p) = \int_{s_i} f(x, y)\, ds_i \tag{7}$$

or is represented in the symbolical form as an integral transform

$$\mathrm{F}(\alpha, p) = \mathrm{R}\left\{f(x, y)\right\}. \tag{8}$$

In the case where the summarized beams are known for the whole set of parameters (α, p), relation (8) admits the inversion

$$f(x, y) = \mathrm{R}^{-1}\left\{F(\alpha, p)\right\} = -\frac{1}{2\pi^2}\int_0^{\pi} d\alpha \int_{-\infty}^{\infty} \frac{F(\alpha, p)\, dp}{(p - p_0)^2}$$

$$= -\frac{1}{2\pi^2}\int_0^{\pi} d\alpha \int_{-\infty}^{\infty} \frac{F'(\alpha, p)\, dp}{(p - p_0)} = -\frac{1}{2\pi^2}\int_0^{\pi} d\alpha \int_{-\infty}^{\infty} F''(\alpha, p) \ln\left|p - p_0\right|\, dp, \tag{9}$$

where F' and F'' are the derivatives averaged over the coordinate p:

$$F'(\alpha, p) = \frac{\partial}{\partial p}\left\{F(\alpha, p)\right\}; \quad F''(\alpha, p) = \frac{\partial^2}{\partial p^2}\left\{F(\alpha, p)\right\}. \tag{10}$$

For a speckle photography, Eq. (9) takes the simple form

$$f(x, y) = \frac{n(x, y) - n_{\infty}}{n_{\infty}} = -\frac{1}{2\pi^2}\int_0^{\pi} d\alpha \int_{-\infty}^{\infty} \frac{\varepsilon_p(\alpha, p)\, dp}{(p - p_0)}, \tag{11}$$

where ε_p is the angle of deflection of the probe radiation in the direction of the coordinate p. In the case where the summarized beams are determined with errors, the integral Radon transform takes the more complex form

$$\hat{f}(x, y) = \widehat{\mathrm{R}}^{-1}\left\{\widehat{\mathrm{F}}(\alpha, p) + \beta\right\}. \tag{12}$$

It is precisely this form of the integral Radon transform that corresponds to experiments, in which there always arise errors in measuring summarized beams. For the axisymmetric function $f(x, y) = f(r)$, the integral Radon transform takes the form of the Abelian transform

$$F(y) = \mathrm{A}\left\{f(r)\right\}, \tag{13}$$

that admits the inversion

$$f(r) = \mathrm{A}^{-1}\left\{F(y)\right\} = -\frac{1}{\pi}\frac{d}{d(r^2)}\int_r^{r_\infty} F(y)\frac{d(y^2)}{\sqrt{y^2 - r^2}} = -\frac{1}{\pi}\int_r^{r_\infty} F'(y)\frac{dy}{\sqrt{y^2 - r^2}}. \tag{14}$$

In the case where the angles of deflection of a probe radiation is recorded, the direct and inverse Abelian transforms take the simpler form

$$\varepsilon(y) = 2y\int_y^{r_\infty}\frac{\partial}{\partial r}\left[\frac{n}{n_\infty}\right]\frac{dr}{\sqrt{r^2 - y^2}}, \quad \frac{n(r) - n_\infty}{n_\infty} = -\frac{1}{\pi}\int_r^{r_\infty}\frac{\varepsilon(y)\,dy}{\sqrt{y^2 - r^2}}. \tag{15}$$

In [51–53], modern possibilities of representation of large-scale vortices in three-dimensional flows with a small asymmetry with the use of a small-aspect tomography based on the high-accuracy digital speckle photography are described, and the calculation and experimental data obtained on three-dimensional flows are compared in Fig. 10. It is shown that the structure of a three-dimensional flow with a small asymmetry can be represented with 10% accuracy with the use of even 3–4 projections. The analysis of flows with a large asymmetry calls for measurements with a larger number of projections.

Conclusions. Modern digital laser technologies and methods of recording images make it possible to accumulate, in the digital form, large arrays of experimental data on rapidly proceeding complex processes, and the mathematical processing of these data with the use of statistical correlation analysis and the integral Abelian and Radon transforms allows one to obtain quantitative information on the local large-scale vortex structure of a flow as a whole. The determination of the local parameters of a small-scale turbulence is a separate problem that can be successfully solved with the use of the integral Erbeck and Merzkirsh transforms [54].

The author expresses his gratitude to Professors W. Merzkirch (Germany) and C. Greated (Great Britain), Doctor U. Kompenhans (Germany), and Doctor of Physics and Mathematics O. G. Penyaz'kov for their attention, useful discussions, and valuable recommendations, Candidates of Science N. V. Bazylev, G. N. Blinkov, D. E. Vitkin, S. M. Vlasenko, E. I. Lavinskaya, and P. P. Khramtsov for support in the performance of experiments and development of mathematical programs for processing of images, Professors J.-B. Saulnier and S. A. Martem'yanov (CNRS6, France) for useful discussions and recommendations as well as the INTAS, the National Academy of Sciences of Belarus, the Belarusian Republic Basic Research Foundation, and the National Center of Scientific Investigations of France for partial financial support of this work in the form of grant for the INTAS projects 05-1000007-425, "Hydrogen-19," "Nanotech 1.13," "Thermal Processes-25," T07F-005, and T07-070.

NOTATION

A, integral Abelian transform; F, summarized beam in integral measurements; F_{s_i}, summarized beam along the trajectory of the ith beam s_i; $\widehat{F}(\alpha, p)$, estimation of the summarized beam; $\mathbb{F}$, Fourier transform; $f(x, y, z)$, distribution of the desired physical quantity in an object; $\hat{f}(x, y)$, estimation of a desired function $f(x, y)$; g, free fall acceleration; h, differential height in the tube of a water pressure guide; I, radiation intensity of a light wave, W/m^2; I_0, radiation intensity of a light wave at the center of a band, W/m^2; p, pressure, Pa; (p, s) and (x, y), rectangular coordinate system; R, integral Radon transform; $\widehat{\mathrm{R}}$, estimation of the integral Radon transform; $\mathbb{R}_{ij}(p, q)$, cross-correlation function of

the images i and j on a matrix with coordinates (p, q); s_i, trajectory of an ith beam; α, projection angle of measurements, rad; ε, angle of deflection of the probe laser radiation, rad; λ, radiation wavelength, m; ν, spatial frequency, m^{-1}; ρ, density, kg/m^3.

REFERENCES

1. A. S. Dubovik, *Photographic Recording of Rapidly Proceeding Processes* [in Russian], Nauka, Moscow (1964).
2. Yu. E. Nesterikhin and R. I. Soloukhin, *Methods of Rapid Measurements in Gas Dynamics and Plasma Physics* [in Russian], Nauka, Moscow (1967).
3. V. F. Klimkin, A. N. Papyrin, and R. I. Soloukhin, *Optical Methods of Recording Rapidly Proceeding Processes* [in Russian], Nauka, Novosibirsk (1980).
4. H. Schardin, Die Schlierenverfaren und ihre Anwendungen, *Naturwissenschaft*, **20**, 303–439 (1949).
5. D. D. Maksutov, *Shadow Methods of Investigating Optical Systems* [in Russian], Gostekhizdat, Moscow (1934).
6. A. S. Abrukov, *Shadow and Interference Methods of Investigating Optical Inhomogeneities* [in Russian], Kazan' (1962).
7. F. J. Weinberg, *Optics of Flame*, Butterworth, London (1963).
8. L. A. Vasil'ev, *Shadow Methods* [in Russian], Nauka, Moscow (1968).
9. T. V. Bazhenova, L. G. Gvozdeva, Yu. S. Lobastov, I. M. Naboko, R. G. Nemkov, and O. A. Predvoditeleva, *Shock Waves in Real Gases* [in Russian], Nauka, Moscow (1968).
10. W. Hauf and U. Grigull, Optical methods in heat transfer, *Adv. Heat Transfer*, **6**, 131–366 (1970).
11. W. Merzkirch, *Flow Visualization*, 2nd ed., Academic Press, Orlando (1987).
12. T. S. Durrani and C. A. Greated, *Laser Systems in Flow Measurements* [Russian translation], Énergiya, Moscow (1980).
13. R. J. Emrich (Ed.), *Methods of Experimental Physics. Fluid Dynamics*, Academic Press, New York (1981).
14. B. S. Rinkevichyus, *Laser Diagnostics of Flows* [in Russian], MÉI, Moscow (1980).
15. O. V. Achasov, N. N. Kudryavtsev, S. S. Novikov, R. I. Soloukhin, and N. A. Fomin, *Diagnostics of Nonequilibrium States in Molecular Lasers* [in Russian], Nauka i Tekhnika, Minsk (1985).
16. F. Maiynger and O. Feldman (Eds.), *Optical Measurements. Techniques and Applications*, 2nd augm. ed., Springer Verlag, Berlin (2002).
17. W. Merzkirch, Flow visualization, in: *Encyclopedia of Physical Science and Technology*, 3rd ed., Vol. 6, Academic Press, Orlando (2002).
18. Yu. N. Dubnishchev, V. A. Arbuzov, P. P. Belousov, and P. Ya. Belousov, *Optical Methods for Investigation of Flows* [in Russian], Sib. Univ. Izd., Novosibirsk (2003).
19. I. A. Znamenskaya, L. G. Gvozdeva, and N. V. Znamenskii, *Methods of Visualization in Mechanics of Gases* [in Russian], MGAI im. S. Ordzhonikidze, Moscow (2001).
20. J. C. Dainty (Ed.), *Laser Speckle and Related Phenomena*, 2nd ed., Springer Verlag, Berlin (1984).
21. N. A. Fomin, U. Werneking, and W. Merzkirch, Speckle photography of a turbulent density field, in: M. Pichal (Ed.), *Optical Methods in Dynamics of Fluids and Solids*, Springer Verlag, Berlin (1985), pp. 159–165.
22. N. Fomin, *Speckle Photography for Fluid Mechanics Measurements*, Springer Verlag, Berlin (1998).
23. M. Raffel, C. E. Willert, and J. Kompenhans, *Particle Image Velocimetry. A Practical Guide*, Springer Verlag, Berlin (1998).
24. N. B. Bazylev, E. I. Lavinskaya, S. P. Rubnikovich, and N. A. Fomin, *Digital Laser Speckle-Anemometry of Flows in Microchannels*, Preprint No. 8 of the Heat and Mass Transfer Institute, National Academy of Sciences of Belarus, Minsk (2006).
25. E. F. C. Somerscales, Measurement of velocity. Tracer methods, in: R. J. Emrich (Ed.), *Methods of Experimental Physics*, Vol. 18A, *Fluid Dynamics*, Academic Press, New York (1981), pp. 1–240.
26. N. B. Bazylev, E. I. Lavinskaya, and N. A. Fomin, Influence of multiple-scattering processes on the laser probing of biological tissues, *Inzh.-Fiz. Zh.*, **76**, No. 5, 16–24 (2003).
27. R. J. Emrich, Measurement of velocity. Probe methods for velocity measurements, in: R. J. Emrich (Ed.), *Methods of Experimental Physics*, Vol. 18A, *Fluid Dynamics*, Academic Press, New York (1981), pp. 241–344.

28. A. A. Maslov, Microflows and microsensors in gas dynamics, *Plenary paper at the 13th Int. Conf. on the Methods of Aerophysical Research*, 5–10 February 2007, Novosibirsk (2007).
29. R. P. Benedict, *Fundamentals of Temperature, Pressure and Flow Measurements*, John Wiley, New York (1969).
30. A. G. Shashkov, *Thermoresistors and Their Application* [in Russian], Nauka, Moscow (1967).
31. R. I. Soloukhin, C. W. Curtis, and R. J. Emrich, Measurement of pressure, in: R. J. Emrich (Ed.), *Methods of Experimental Physics*, Vol. 18A, *Fluid Dynamics*, Academic Press, New York (1981), pp. 499–610.
32. S. G. Zaitsev, On measurement of rapidly varying pressures in a gas medium, *Prib. Tekh. Éksp.*, No. 6, 96–99 (1958).
33. R. I. Soloukhin, Pulse pressure-sensitive detector, *Prib. Tekh. Éksp.*, No. 3, 170–171 (1961).
34. V. I. Zagorel'skii, N. N. Stolovich, and N. A. Fomin, Pulsed piezoelectric transducer with a matching amplifier for measurement of rapidly varying pressures, *Inzh.-Fiz. Zh.*, **42**, No. 2, 303–306 (1982).
35. G. M. Zharkova, V. N. Kovrizhina, A. P. Petrov, B. V. Smorodsky, H. Khauss, T. Roediger, S. Wagner, and E. Fraemer, Comparative heat transfer studies at hypersonic conditions by means of three measurement techniques. Measurement technique, experimental setup and preceding investigations, in: *Proc. 13th Int. Conf. on the Methods of Aerophysical Research*, Novosibirsk, Parallel (2007), Pt. 1, pp. 221–228.
36. R. Konrath, C. Klein, A. Schroder, and J. Kompenhans, Combined application of pressure sensitive paint and particle image velocimetry to the flow above a delta wing, in: I. Grant (Ed.), *Flow Visualization*, CD Rom *Proc. 12th Int. Symp. on Flow Visualization*, Optimage Ltd., Edinburgh (2006), pp. 1–14.
37. N. Fujisawa, N. Nakano, and Y. Oguma, Wind tunnel studies of shear-stress measurements by liquid crystal coatings, in: I. Grant (Ed.), *Flow Visualization*, CD Rom *Proc. 12th Int. Symp. on Flow Visualization*, Optimage Ltd., Edinburgh (2006), pp. 1–9.
38. D. C. Reda, M. C. Wilder, D. J. Farina, and G. Zilliac, New methodology for the measurement of surface shear stress vector distributions, *AIAA J.*, **35**, 608–614 (1997).
39. G. Ben-Dor, O. Igra, and T. Elperin (Eds.), *Handbook of Shock Waves*, Vol. 1, Academic Press, New York (2001).
40. G. S. Settles, *Schlieren and Shadowgraph Techniques. Visualizing Phenomena in Transparent Media*, Springer Verlag, Berlin (2001).
41. M. Hugenschmidt and K. Volrath, Light sources and recording methods, in: R. J. Emrich (Ed.), *Methods of Experimental Physics*, Vol. 18A, *Fluid Dynamics*, Academic Press, New York (1981), pp. 687–753.
42. N. A. Fomin and R. I. Soloukhin, Gasdynamic problems for optically inverse media, *Revue de Phys. Appl.*, **14**, No. 2, 421–437 (1979).
43. R. I. Soloukhin and N. A. Fomin, *Gasdynamic Mixing Lasers* [in Russian], Nauka i Tekhnika, Minsk (1984).
44. N. A. Fomin, *Speckle Photography of Gas Flows* [in Russian], Nauka i Tekhnika, Minsk (1989).
45. C. E. Willert and M. Gharib, Digital particle image velocimetry, *Exp. Fluids*, **10**, No. 4, 181–193 (1991).
46. R. J. Adrian, Particle-imaging techniques for experimental fluid mechanics, *Annual Rev. Fluid Mech.*, **23**, 261–304 (1991).
47. J. Westerweel, *Digital Particle Image Velocimetry: Theory and Application*, PhD Dissertation, Delft University Press, Delft (1993).
48. W. Merzkirch, T. Mrozewski, and H. Wintrich, Digital particle image velocimetry applied to a natural convective flow, *Acta Mechanika* (Suppl.), **4**, 19–26 (1994).
49. A. Asseban, M. Lallemand, J.-B. Saulnier, N. Fomin, E. Lavinskaya, W. Merzkirch, and D. Vitkin, Digital speckle photography and speckle tomography in heat transfer studies, *Optics Laser Technol.*, **32**, 583–592 (2000).
50. N. B. Bazylev, S. M. Vlasenko, E. I. Lavinskaya, and N. A. Fomin, Digital speckle photography of rapidly proceeding processes in the quasi-real time, *Dokl. Nats. Akad. Nauk Belarusi*, **45**, No. 5, 55–59 (2001).
51. N. B. Bazylev, A. M. Bratchenya, E. I. Lavinskaya, S. A. Martem'yanov, and N. A. Fomin, Digital laser anemometry of flows in the microchannels of hydrogen-power fuel cells, *Dokl. Nats. Akad. Nauk Belarusi*, **49**, No. 5, 124–129 (2005).

52. E. I. Lavinskaya, S. A. Martem'yanov, J.-B. Saulnier, and N. A. Fomin, Small-aspect-angle laser tomography of complex gasdynamic flows, *Inzh.-Fiz. Zh.*, **77**, No. 5, 94–104 (2004).
53. N. Fomin, E. Lavinskaya, and K. Takayama, Limited projections laser speckle tomography of complex flows, *Optics Lasers Eng.*, **44**, No. 3–4, 335–349 (2006).
54. N. Fomin, E. Lavinskaya, and D. Vitkin, Speckle tomography of turbulent flows with density fluctuations, *Exp. Fluids*, **33**, 160–169 (2002).